Evaluation of Combustion Models for High Speed H$_2$/Air Confined Mixing Layer Using DNS Data

DEBASIS CHAKRABORTY,*[†] P. J. PAUL, and H. S. MUKUNDA
Department of Aerospace Engineering, Indian Institute of Science, Bangalore 560 012, India

The capability of empirical combustion models to predict the mean reaction rate for supersonic mixing layer is evaluated by using the stored time series data of direct numerical simulations (DNS). The confined supersonic H$_2$/air mixing layer—the prototype representation of the scramjet combustor flow field—is taken as the test case. The reaction rate profiles of various species obtained from the DNS results are compared with the reaction rate profiles obtained from these combustion models. The combustion models based on fast chemistry approximation are seen to predict the peak mean reaction rate much higher (about two orders of magnitude) compared to DNS data, particularly in the mixing layer region where the reaction is taking place. The Eddy Dissipation Concept (EDC) based combustion models for finite rate chemistry suggested by Magnussen and coworkers predict the mean reaction rate of all the major and minor species extremely well. The EDC model with detailed full chemistry (FC) and finite rate single-step chemistry (SSC) captures all essential features of reaction rate profile distribution with similar order of magnitude peak values, although a thinner reaction zone is predicted. The comparisons of mean reaction rates with different hydrogen and air stream temperatures reveal that the model can predict the mean reaction rate for practical scramjet combustor flow field. The model is also seen to predict the mean reaction rate well at a location close to the occurrence of ignition. A modification of this model allowing a nonunity Schmidt number, a feature very important for the flow involving hydrogen, shows little improvement in the prediction of the reaction rates. It is inferred that for hypervelocity reactive flows for which heat release due to chemistry is counteracted by significant enthalpy change due to gas dynamics, the finite rate EDC model with fine tuning for reaction zone width may be adequate to describe full chemistry effect.   © 2000 by The Combustion Institute

INTRODUCTION

The prediction of turbulent reactive flow in the scramjet combustor flow field largely depends on the proper choice of the combustion model. Modeling turbulent combustion continues to be a major challenge in aerospace applications. The major difficulty in modeling turbulence–chemistry interaction in reacting flows is due to the fact that the mean production rate given by chemical kinetics is a highly nonlinear function of several fluid dynamical and chemical variables. Due to nonlinearity, the mean value of the production rate of the species is not the value of the production rate obtained from the mean variables. Our understanding of the various processes taking place in a turbulent reacting flow field has improved considerably with the advent of direct numerical simulation (DNS), where the full Navier-Stokes equation is solved exactly along with the species continuity equations including chemistry by resolving the time and length scale adequately. Givi [1] and Vervisch and Poinsot [2] summarize much of the interesting findings from DNS of reacting flows. Although a very useful learning tool, the model-free simulation for reacting flow is possible only for a simple flow. The search for a proper modeling of mean reaction rate is still a challenge.

Several approaches are proposed in the literature. In the Moment Closure Method [3–5], the exponential term in the Arrhenius equation is expanded in a series, and the higher order terms are truncated. Truncation of the higher order terms gives erroneous result if the species and temperature fluctuations are significant compared to their mean values and this severely limits the validity of this approach. Among the empirical models, Spalding [6] proposed a very simple but very useful formula for calculating the mean reaction rate of the fuel—the Eddy Break Up (EBU) model. The development of the model is based on the assumption that the rate of burning depends upon the rate at which the fragments of unburned gases are broken

---

*Corresponding author. E-mail: v_adimurthy@vssc.org
[†]Scientist/Engineer, Aerodynamics Division, VSSC, Thiruvananthapuram.

into smaller fragments by the action of turbulence, and the rate of reaction is supposed to be proportional to the rate of decay of turbulence energy. The Eddy Dissipative Concept (EDC) set forth by Magnussen and Hjertager [7] gives an empirical expression for the mean reaction rate based on the assumption that chemical reaction occurs in an isolated region where the dissipation of turbulent energy is significant. Recently Gran [8] gave the formulation for reaction rates for finite rate chemistry based on the eddy dissipation concept. The applicability of these models is limited todate to low-speed flows only. Although the probability density function (pdf) method [9, 10] is theoretically sound and the chemical reaction term does not need any modeling, the method is not completely model-free. The pdf transport equation has to be coupled with classical turbulence models and all important turbulent scalar diffusion processes need to be modeled. The case of a steady one- or two-dimensional parabolic flow with a simple chemical scheme is tractable, but for two- or three-dimensional elliptic flow with a large number of chemical variables with a complex chemical scheme, the situation is very difficult. In the presumed pdf method [11–13] an approximate shape for the pdf is assumed depending on few parameters. These parameters are calculated based on the balance equation for the first few moments. Unfortunately, most of the assumed pdf in the literature so far have been reasonable only during certain stages of the mixing process and are quite unrealistic at other stages.

It is clear that the development of the combustion models for high-speed reactive flows is in a formative stage. The use of empirical models for the prediction of the mean reaction rate in turbulent flows can be very helpful. Evaluation of these combustion models from DNS data is an important task, since such an evaluation can bring out the advantages and shortcomings of these models before they are put to regular use. In this paper the time series data of DNS [14, 15] of confined reacting mixing layer (which represents the scramjet combustor flow field) are used to evaluate the applicability of empirical combustion models for the prediction of mean reaction rate for hypersonic combustion.

DNS CALCULATION—THE CODE AND THE COMPUTATIONAL DETAILS

In order to understand the combustion process inside the scramjet combustor, DNS were performed for the confined supersonic reacting mixing layer as it contains all the fundamental processes involved in supersonic combustion in a confined environment. The results of the DNS calculations for the H_2/air confined supersonic mixing layer are given in the earlier work of the present authors [14, 15]. Three different conditions were simulated. In the first case, the simulation is performed for the hypervelocity mixing layer experiment of Erdos et al. [16]. In this experiment, the secondary stream (H_2) comes in contact with the primary stream (air) at the edge of the splitter plate in an enclosed test section of size 535 mm $\times$ 25.4 mm. The Mach number and the temperature of the two streams are 3.99 and 2400 K (air) and 3.09 and 103 K (H_2) respectively. The convective velocity is 3000 m/s and the convective Mach numbers are 0.85 and 0.82 referred to H_2 and air streams respectively. The free shear layer experiments of Clemens and Mungal [17] suggest dominant three-dimensional effects for this convective Mach number range and have been supported by linear instability analyses [18, 19] which have shown that oblique disturbances become more and more unstable as convective Mach number exceeds 0.6. However, Tam and Hu [20] and Zhuang et al. [21] have shown that, for laterally confined mixing layers, the most unstable mode is the lowest order two-dimensional mode.

The principal point made in these papers is that the coupling between the motion of the shear layer and the channel acoustic wave produces a new instability mechanism in the supersonic range which originates from the wall confinement and is different from the classical Kelvin-Helmholtz instability. Zhuang et al. [21] have shown that the bounded two-dimensional modes are in good agreement with the experiments of Papamoschou and Roshko [22]. Lu and Wu [23] have performed two-dimensional simulations for a mixing layer with a convective Mach number as high as 1.77 citing the work of Tam and Hu [20] who studied the effect of confinement on the shear layer development in supersonic streams. These studies have shown

TABLE 1

Inflow Parameters of the Cases with Various Stream Temperatures

Cases	Chemical Kinetics	Species	u (km/s)	T (K)	M	p (MPa)
Case 1	FC	H_2	2.4	103	3.09	0.021
		Air	3.8	2344	3.99	0.021
	SSC	H_2	2.4	103	3.09	0.021
		Air	3.8	2344	3.99	0.021
Case 2	FC	H_2	2.4	1200	5.63	0.021
		Air	3.8	1200	0.92	0.021
Case 3	FC	H_2	2.4	1500	5.06	0.021
		Air	3.8	1500	0.83	0.021

that two-dimensional simulation is satisfactory for confined mixing layers. Apart from confinement effect, heat release effect also plays a vital role to make the most unstable mode two-dimensional. The linear stability analysis of reacting compressible mixing layer by Shin and Ferziger [24] has demonstrated that heat release makes the dominant mode two-dimensional even in the high Mach number region; they have concluded that the most unstable mode for reacting flow is two-dimensional even if the instability mode is three-dimensional (oblique) for the nonreacting case.

In the present work, both confinement and heat release effects are part of the physics implying that the role of large scale two-dimensional structures in modulating the chemistry–flow interactions is significant and can be understood from two-dimensional simulations.

As the experimental condition is far removed from the scramjet operating condition, especially with regard to the temperature of the streams, two more simulations were made by taking realistic stream temperatures. In these simulations, both the primary and secondary streams have the same temperature 1200 K and 1500 K respectively, while all other properties are kept same at the inflow plane. The details of the inflow parameters of all the calculations are shown in Table 1. The code used in the DNS is the SPARK2D combustion code developed at the NASA Langley Research Center (LaRC) by Drummond et al. [25] and has already been used in Sekar and Mukunda [26] and Mukunda [27]. It uses a fourth-order compact MacCormack scheme with second-order temporal accuracy. This choice represents a compromise be-

tween the accuracy of higher order numerical algorithms and the robustness and efficiency of lower order methods. The code has been validated by computing a linearly unstable shear flow problem in the early stages of the growth. Carpenter and Kamath [28, 29] have demonstrated that, with the compact schemes considered here, the growth rates with the initial profiles based on the eigenfunctions predict those from linear stability theory for free shear layers to within 1% for a time duration equal to about five times the sweep time of the flow field. This accuracy is adequate for the present computations needing a maximum of three sweep times—one sweep for clearing the flow field, and two more sweeps to collect statistical information and also to check on the statistical invariance of the calculations.

The reaction rates for the first case are calculated using both single-step chemistry (SSC) and full chemistry (FC) kinetics whereas for the second and third cases only FC kinetics is used. A reaction mechanism involving seven species and seven reversible reactions [25, 26] has been chosen for the FC calculations. This reaction mechanism include the species H_2, O_2, H_2O, OH, H, O, and N_2. The species HO_2, and H_2O_2, important in ignition are not included in the mechanism. This is because the present study is aimed at examining combustion modeling. The reaction steps and the rate parameters of the reactions are given in Table 2. For SSC calculations, the following reversible reaction has been chosen.
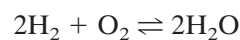
$$2H_2 + O_2 \rightleftharpoons 2H_2O$$

TABLE 2

Elementary Reactions and Reaction Rate Parameters Used for Full Chemistry
Computations

No.	Reaction	A	N	E/R, K
1	$H_2 + O_2 \rightarrow OH + OH$	0.170×10^{14}	0	24230
2	$O_2 + H \rightarrow OH + O$	0.142×10^{15}	0	8250
3	$H_2 + OH \rightarrow H_2O + H$	0.316×10^{08}	1.8	1525
4	$H_2 + O \rightarrow OH + H$	0.207×10^{15}	0	6920
5	$OH + OH \rightarrow H_2O + O$	0.550×10^{14}	0	3520
6	$OH + H + M \rightarrow H_2O + M$	0.221×10^{23}	-2	0
7	$H + H + M \rightarrow H_2 + M$	0.655×10^{18}	-1	0

and the net rate of reaction of H_2 (in kg-mol/m^3 s) is given by the expression [25, 26]

$$\frac{dc_{H_2}}{dt} = -2[1.102 \times 10^{19}$$

$$\cdot \exp(-8052/T)c_{H_2}^2 c_{O_2} - k_b c_{H_2O}^2] \qquad (1)$$

where c is the molar concentration (in g-mol/cm^3) and k_b, the rate constant of the reverse reaction, is obtained from the forward rate constant and equilibrium constant.

The boundary conditions set for the present problem are as follows: The no slip conditions and constancy of wall temperature are imposed on the wall. On the inflow stream velocity fluctuations are imposed over a range of frequencies at total rms intensity of 0.3% of the mean velocity. The frequency has been normalized with the mean velocity to channel width ratio. The frequency range allows the mixing layer to grow as may happen in reality. The exit boundary condition is obtained by second-order extrapolation and is considered satisfactory for this problem dominated by supersonic flow.

The calculation used a 1000×101 grid with grid stretching at high gradient zones—near interface, near splitter plate, and near the walls. The grid independence of the results was established [14] by not only comparing the result of the simulation with different grids but also comparing the spectral content of fluctuation with different grids.

COMBUSTION MODELING

Chemical reactions take place when reactants are mixed on a molecular scale at sufficiently high temperature. In turbulent flow, the molecular mixing is associated with the smallest scale of turbulence and the process of molecular mixing is similar to the dissipation of turbulent kinetic energy. In this paper we will discuss the following empirical combustion models for predicting the mean reaction rates: (1) EBU model; (2) EDC with fast chemistry limit; (3) EDC for finite rate chemistry for both SSC and FC.

EBU Model

The rate of consumption of fuel $\overline{\dot{w}}_f$ modeled on the basis of the EBU model [6] as

$$\overline{\dot{w}}_f = -A_1 \bar{\rho} \tilde{Y}_L \frac{\epsilon}{k} \qquad (2)$$

where overbars indicate the ensemble (Reynolds) averages and tildes indicate mass weighted (Favre) averages. As usual ρ, k, ϵ represent density, turbulent kinetic energy, and the rate of dissipation of turbulent kinetic energy. $\tilde{Y}_L = \min(\tilde{Y}_f, \tilde{Y}_{OX}/s)$ is the limiting reactant mass fraction, $\tilde{Y}_f$ and $\tilde{Y}_{OX}$ are the fuel and the oxidizer mass fraction, and s is the stoichiometric ratio.

Bilger [30] has proved theoretically that for mixing limited reaction, the mean production rate is proportional to the pdf of the mixture fraction at stoichiometry. Assuming different shapes of pdf, namely, clipped Gaussian, Beta, and Gamma functions, Brizuela and Bilger [31] have proposed an empirical expression for the mean reaction rate

$$\overline{\dot{w}}_f = A_1^* \bar{\rho} \frac{\epsilon}{k} Y_B \check{Y}_f^m \check{Y}_{OX}^{-n} \left(\frac{1}{\check{Y}_f} + \frac{1}{\check{Y}_{OX}} \right)^{-p} \qquad (3)$$

where Y_B is a constant and $\check{Y}_f = \tilde{Y}_f/Y_B$ and $\check{Y}_{OX} = \tilde{Y}_{OX}/sY_B$. The values of the constants m, n, p, and A_1^* are tabulated in Ref. 31 for the different shapes of pdf. For the stoichiometric mixture fraction 0.03 considered in this study, the values of the variables are $A_1^* = 7.0$, $m = 0.8$, $n = 0.6$, and $p = 1.1$ [31].

Once the mean production rate for the fuel is obtained, the mean production rate for the oxidizer and the product is obtained from

$$\overline{\dot{w}_{OX}} = s\overline{\dot{w}_f} \tag{4}$$

$$\overline{\dot{w}_p} = (1 + s)\overline{\dot{w}_f} \tag{5}$$

EDC

Fundamental Aspects

EDC gives an empirical expression for the mean reaction rate based on the assumption that chemical reaction occurs in the regions where the dissipation of the turbulent energy is significant. In flows of moderate to intense turbulence, these regions are concentrated in isolated highly strained regions, occupying only a small fraction of the flow. These regions consist of fine structure whose characteristic dimensions are of the order of Kolmogorov length scale in one or two dimensions but not in the third [32, 33]. The fine structures are responsible for the dissipation of turbulence into heat. Within these structures one can assume that the reactants are mixed on a molecular scale.

Magnussen and coworkers [7, 8] proposed the following expression for the mean reaction rate for the finite rate chemistry.

$$\frac{\overline{\dot{w}_i}}{\rho} = \frac{\gamma^2 \chi}{\tau^*} (Y_i^0 - Y_i^*) \tag{6}$$

where γ is the fraction of the flow occupied by the fine structure region and is modeled as:

$$\gamma = \left(\frac{3C_{D2}}{4C_{D1}^2}\right)^{1/4} \left(\frac{\nu^* \tilde{\epsilon}}{\bar{k}^2}\right)^{1/4} \tag{7}$$

where $C_{D1} = 0.134$ and $C_{D2} = 0.5$ are model constants and ν is the kinematic viscosity. Alternatively γ can be expressed as $\gamma = 3.43/\sqrt{Re_\lambda}$,

where $Re_\lambda = \sqrt{(20k^2)/(3\nu\epsilon)}$ is the Reynolds number based on Taylor length scale.

The time scale for the mass transfer between the fine structures and the surroundings (τ^*) is estimated as

$$\tau^* = \left(\frac{C_{D2}}{3}\right)^{1/2} \left(\frac{\nu^*}{\epsilon}\right)^{1/2} \tag{8}$$

χ is the fraction of the fine structures where reaction occurs. Gran [8] demonstrated that the assumption $\chi = 1$ leaves the results almost unaltered. In our analysis the value of χ will be considered as unity. The superscripts $*$ and 0 refer to the fine structure and the surrounding fluids respectively. The fine structure is treated as constant-pressure homogeneous reactor where effects of finite rate chemical kinetics are taken into account. The properties of constant-pressure homogeneous reactor are assumed to be time dependent but without any spatial gradient. The set of governing equation for such a reactor is

$$\frac{dh}{dt} = 0 \tag{9}$$

$$\frac{dp}{dt} = 0 \tag{10}$$

$$\frac{dY_i}{dt} = \frac{w_i}{\rho} + \frac{1}{\tau^*} (Y_i^m - Y_i) \qquad i = 1, \cdots ns \tag{11}$$

where the superscript m refers to the fluid entering the reactor. The steady-state solution of Eq. 11 gives the fine structure state. The reaction rate w_i can be obtained from Eq. 1 or Table 2 depending on whether it is SSC or FC kinetics. The mass fraction of the surrounding fluid Y_i^0 is determined from

$$Y_i^0 = \frac{\bar{Y}_i - \gamma^3 Y_i^*}{1 - \gamma^3} \tag{12}$$

Putting Eq. 6 in the nondimensionalized form we get,

$$R_i = \frac{\dfrac{\overline{\dot{w}_i} k}{\rho\epsilon}}{\bar{Y}_i - Y_i^*} = \frac{11.17}{1 - \gamma^3} \tag{13}$$

Fast Chemistry Limit

The fast chemistry limit is obtained by assuming that there is sufficient time to achieve equilibrium in the fine structures. It is assumed that the reaction can be suitably represented by the single one-step infinite-rate irreversible reaction.

1 kg fuel(f) + s kg oxidant(ox) $\rightarrow$

$$(1 + s) \text{ kg product(P)} \qquad (14)$$

The following set of scaled mass fractions is introduced to simplify the model expressions:

$$\hat{Y}_f = \frac{\bar{Y}_f}{1} \qquad (15)$$

$$\hat{Y}_{ox} = \frac{\bar{Y}_{ox}}{s} \qquad (16)$$

$$\hat{Y}_P = \frac{\bar{Y}_P}{1 + s} \qquad (17)$$

and

$$\hat{Y}_{min} = \min[\hat{Y}_f, \hat{Y}_{ox}] \qquad (18)$$

Magnussen [32] suggests the following model for χ

$$\chi = \chi_1 \cdot \chi_2 \cdot \chi_3 \qquad (19)$$

where χ_1 is the probability of coexistence of the reactants

$$\chi_1 = \frac{(\hat{Y}_{min} + \hat{Y}_P)^2}{(\hat{Y}_f + \hat{Y}_P)(\hat{Y}_{ox} + \hat{Y}_P)} \qquad (20)$$

χ_2 expresses the degree of heating

$$\chi_2 = \min\left[\frac{\hat{Y}_P}{\gamma(\hat{Y}_P + \hat{Y}_{min})}, 1\right] \qquad (21)$$

and χ_3 limits the reaction due to lack of reactants

$$\chi_3 = \min\left[\frac{\gamma(\hat{Y}_P + \hat{Y}_{min})}{\hat{Y}_{min}}, 1\right] \qquad (22)$$

With these expressions for χ, the constraint $0 \leq \chi \leq 1$ is always satisfied. The reaction rate, Eq. 6, can now be written as

$$\frac{\bar{w}_f}{\rho} = -\frac{\gamma^2 \chi_1}{\tau^*} \min[\hat{Y}_{min}, \hat{Y}_P, (\hat{Y}_{min}$$

$$+ \hat{Y}_P)\gamma] \frac{1}{1 - \gamma^3 \chi} \qquad (23)$$

The factor $1/(1 - \gamma^3 \chi)$ is generally very close to unity.

Modifications on EDC Model

The important coefficients involved in momentum, energy, and species transport are viscosity, thermal conductivity, and diffusivity respectively. The transport of species from the surrounding fluid to fine structure is essentially dependent on diffusion process. In the EDC model Eq. 6, τ^* is modeled as $0.4082\sqrt{\mu/\rho\epsilon}$. The fraction of the flow occupied by the fine structure region (γ) is modeled as $2.135\ (\rho k^2/\mu\epsilon)^{-0.25}$. Both these parameters are function of μ in addition to k and ϵ. For reactions involving H_2 and air, various species will have different diffusivities. It is important to bring explicit dependence of mean reaction rate on the diffusivity in place of molecular viscosity. Although it is desirable to take different diffusivities for different species in the mean reaction rate equation, as a first step we consider equal diffusivity of all the species. We propose the following modification in modeling τ^* and γ as:

$$\tau^* = 0.4082 \sqrt{\frac{D}{\epsilon}} \qquad (24)$$

$$\gamma = 2.135 \left(\frac{k^2}{D\epsilon}\right)^{-0.25} \qquad (25)$$

These modifications bring explicit dependence of diffusivity in the mean reaction rate equation.

RESULTS AND DISCUSSION

The details of the DNS of H_2/air confined mixing layer are explained in the previous section. After the solution has attained statistical steady state, several variables such as density, velocities, the mass fractions, and instantaneous reaction rates of all the species were stored at all time steps over one sweep of calculation at all the lateral points of two neighboring axial stations where the flow is well developed. One sweep is taken as the time the flow takes to cross the test section with its convective velocity. The
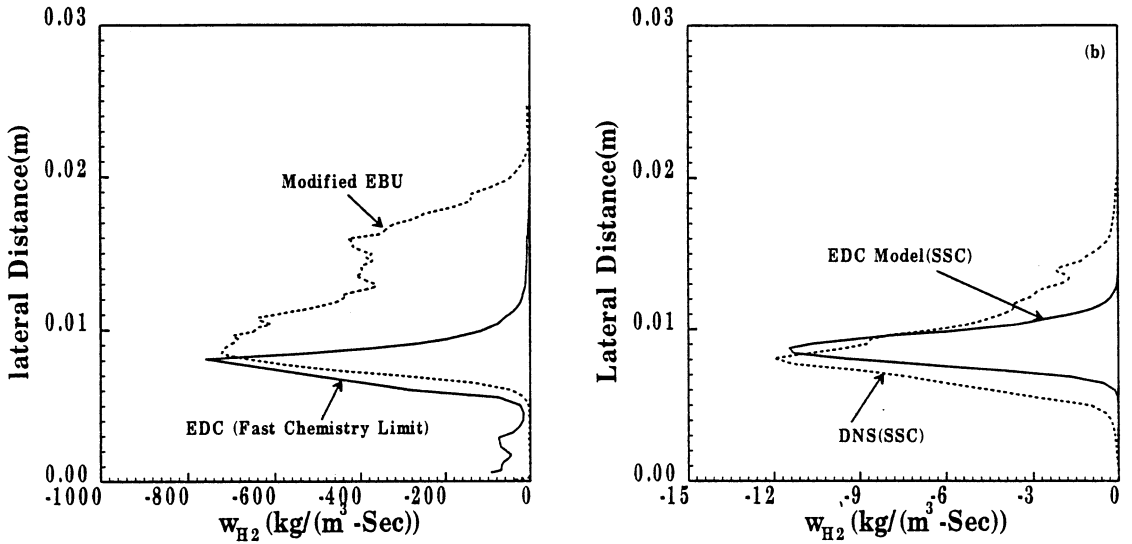
Fig. 1. Comparison of models and DNS data for H_2 reaction rate profile $x = 0.5$ m. (a) between EBU and EDC (fast chemistry limit), (b) between EDC (SSC) and DNS (SSC).

first axial station is chosen at the distance of 0.5 m of the splitter plate and the second axial station is just adjacent to it. From the stored data, the average values of the density (ρ), turbulent kinetic energy (k), rate of dissipation of turbulent kinetic energy (ϵ), and the mass fractions of the species are calculated. With these calculated mean profiles, the mean reaction rates of the fuel (H_2) are calculated for the EBU model with Bilger modifications from Eq. 3, while Eq. 23 is used for calculating mean reaction rate for EDC fast chemistry limit. The mean reaction rates of the species H_2, O_2, and H_2O have also been calculated for EDC (SSC) from Eq. 6. The values of Y_i^* required for the calculation are obtained by integrating Eq. 11 and the values of w_i are obtained from the SSC kinetics Eq. 1. The calculated mean reaction rates of H_2 from the EBU model and EDC (fast chemistry limit) are compared in Fig. 1a and the mean reaction rate obtained from EDC (SSC) compared in Fig. 1b with DNS (SSC) solution at the axial location of 0.5 m from the splitter plate for Case 1. The reaction rate profile of DNS is obtained from the averaging of the stored instantaneous H_2 reaction rates. As expected, the fast chemistry results (both for EBU and EDC [fast chemistry limit]) predict much higher reaction rate compared to DNS solu-

tions. In the mixing layer region, where the reaction takes place, the reaction rate predicted by fast chemistry is about two orders of magnitude higher than the DNS data. The modified EBU model due to Bilger [31] shows a much broader profile than the EDC (fast chemistry limit). The predicted reaction rate with EDC (SSC) matches fairly well with the DNS data. The peak values and the shape of the reaction rate profile obtained from EDC (SSC) and the DNS match closely, although a thinner reaction zone is predicted by EDC (SSC). Mean reaction rate profiles for the species O_2 and H_2O are compared in Fig. 2. As in the case of H_2, the mean reaction rates of O_2 and H_2O predicted by EDC (SSC) match fairly well with the DNS data.

The necessity of using detailed chemistry for simulating high-speed H_2/air mixing layer has been demonstrated in Ref. 14, which revealed that SSC predicts much higher temperature compared to FC. This is mainly because of the absence of any heat absorbing reaction path in SSC. The high temperature present in SSC simulation impedes the growth of the mixing layer. To illustrate the point further, we analyze from DNS data a parameter I which is the measure of unreactedness of the mixed fluid and is defined as:
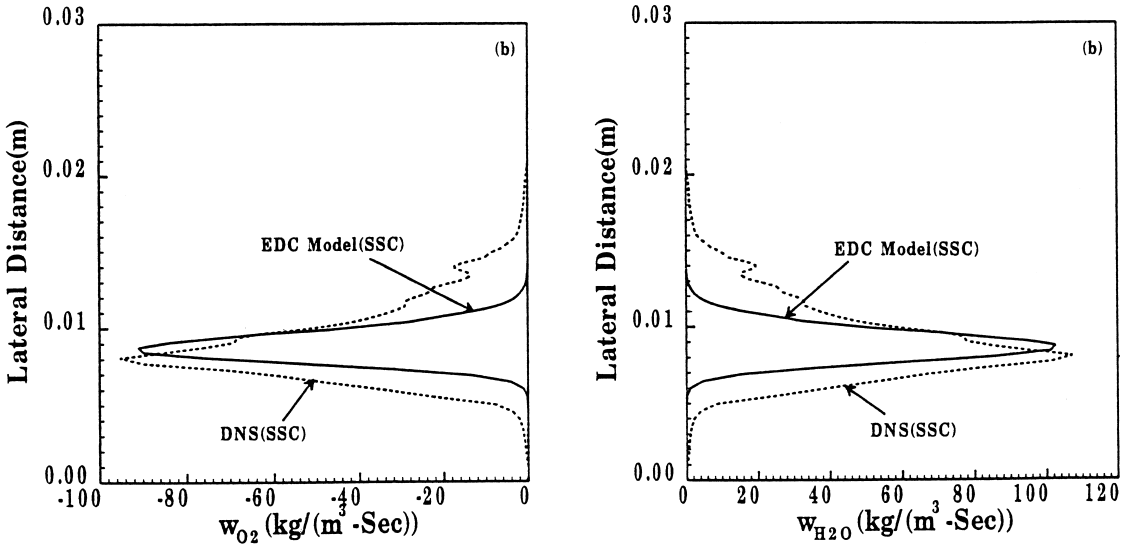
Fig. 2. Comparison of reaction rate profile between EDC (SSC) and DNS (SSC) at x = 0.5 m (a) O_2, (b) H_2O.

$$I = \frac{\int_0^L (Y_{H_2} Y_{O_2})/(Z_H Z_O)\, dy}{\int_0^L dy} \qquad (26)$$

where Z_H and Z_O are the element mass fractions of H and O, whereas Y_{H_2} and Y_{O_2} are H_2 and O_2 mass fractions respectively. Axial variation of time averaging of I is presented in Fig. 3.
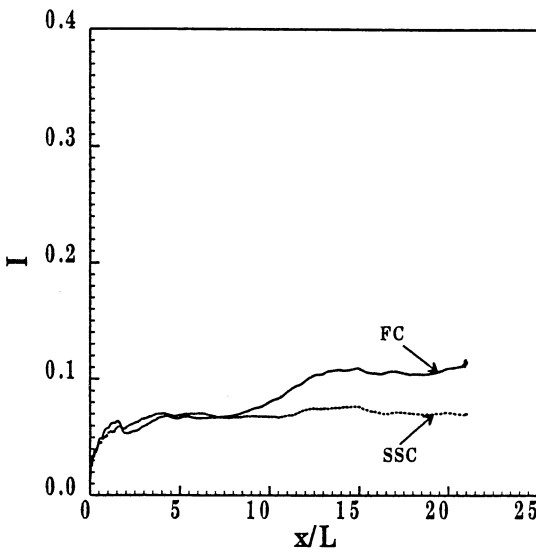

Fig. 3. Axial variation of I.

Axial distance is nondimensionalized by L (=0.0254 μm) − the width of the test section. It is very clear from the figure that SSC is faster than FC. Also for the cases considered, reaction is yet to be completed. Axial variation of I indicates that combustion is reaction-dominated rather than diffusion-limited. In order to assess this issue, instantaneous variation of w'''_{H_2O}/ρ, $Z_H Z_O$, $Y_{H_2} Y_{O_2}$, and T with lateral distance at x = 0.5 m is shown in Fig 4. There are several interesting features that can be derived from the plot. Even though fuel and oxidizer are available, reaction does not occur in most places as the temperature is quite low in most places. Reaction therefore occurs in smaller zones. The width of the reaction zone varies from 2.5 to 3 mm and is covered by at least 15 grid points. The range of $(\dot{w}'''_{H_2O}/\rho)$ is between 15,000 s^{-1} to 12,000 s^{-1}. This implies that the reaction time is of the order 50 to 70 μs. The residence time can be estimated as follows. The vortical structures are typically 30 mm and the flow velocity 3000 m/sec. This give a flow time of 10 μs. The Damköhler number is 0.15–0.2. This is indicative of chemistry-dominated flow. Another way of understanding the behavior is to look at the reaction width. The reaction zone is typically 2.5 mm and the mixed zone is about 20 mm. This implies that mixing has not limited the reaction.

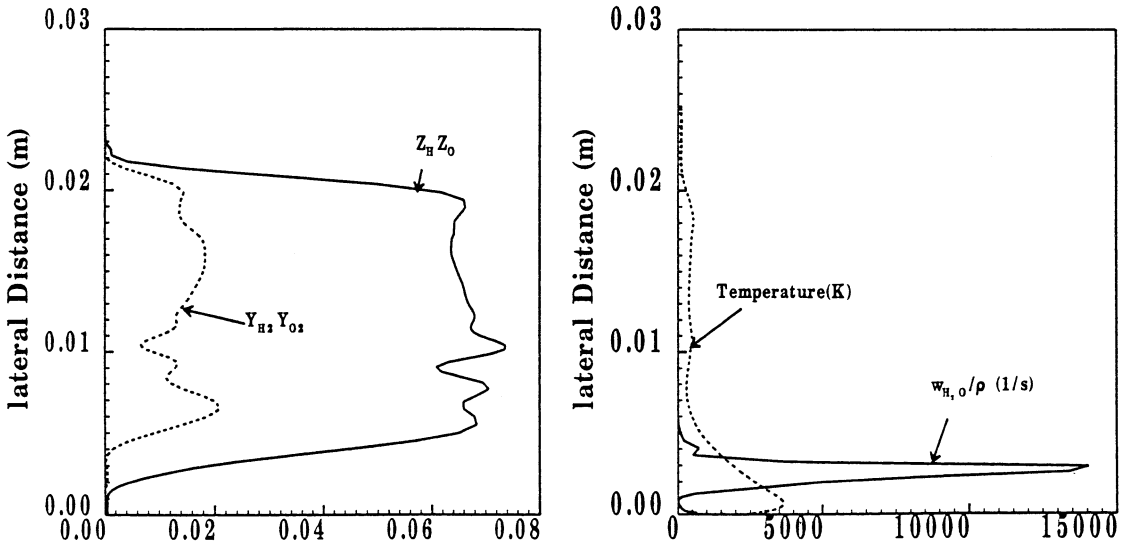Mean reaction rate profiles of various species

Fig. 4. Instantaneous profiles of DNS results for case 1 (a) $Y_{H_2}Y_{O_2}$ and $Z_H Z_O$, (b) $\dot{w}'''_{H_2O}/\rho$, and temperature at $x = 0.5$ m.

obtained from the DNS results are compared with those obtained from the EDC model with FC. The stored time series data from three sets of DNS calculations of confined mixing layer with FC kinetics are used for this purpose. The details of inflow parameters of these DNS calculations are the same as in Table 1. The first case, the H_2/air confined mixing layer, corresponds to the experimental condition of Erdos et al. [16]. In the second case, the temperatures of both the air and H_2 streams are considered 1200 K while maintaining all the other conditions identical. In the third case the temperatures of both the streams are taken as 1500 K. As earlier, the fluid dynamical parameters, the mass fractions, and the instantaneous reaction rates of the species are stored over one sweep at all lateral locations of the two neighboring axial stations at a distance of 0.5 m from the splitter plate. From the stored data, we first determine the mean profiles of k, ϵ, and the species mass fractions. The mean reaction rates of various species were then determined from the EDC (FC) model (Eq. 6) and the modified EDC (FC) model as described in the previous section. The values of Y_i^* required for the calculation are obtained by integrating Eq. 11, and the values of w'''_i are obtained from the FC kinetics given in Table 2. The species production rates thus obtained are compared with the averages of the instantaneous species production rate obtained from the model-free simulation.

The comparisons of H_2 and O_2 production rate profiles obtained from these two approaches for the first case (Erdos experiment case) are presented in Fig. 5 for the axial location of 0.5 m from the splitter plate. It is interesting to note that several peaks and humps present in the DNS result are also picked up by the model. The peak value obtained from the model is about 15% higher than that obtained from the DNS result. The model predicts a thinner reaction zone compared to the DNS result. The species production rate profile comparisons for H_2O and OH are presented in Fig. 6. As in the earlier figure, the shapes of the two curves are similar and the peak values compare well with a thinner reaction zone predicted by the model. Results obtained from the modified EDC (FC) model show a small improvement over the original EDC (FC) model. Similar conclusions can be drawn from the reaction rate profile comparisons of the other minor species O and H as well (not presented here for the sake of brevity).

The comparisons of mean reaction rate profiles of the species H_2, O_2 for case 2 are presented in Fig. 7. For H_2 profile, the model predicts a better comparison for the lower side (air) of the mixing layer whereas the compari-
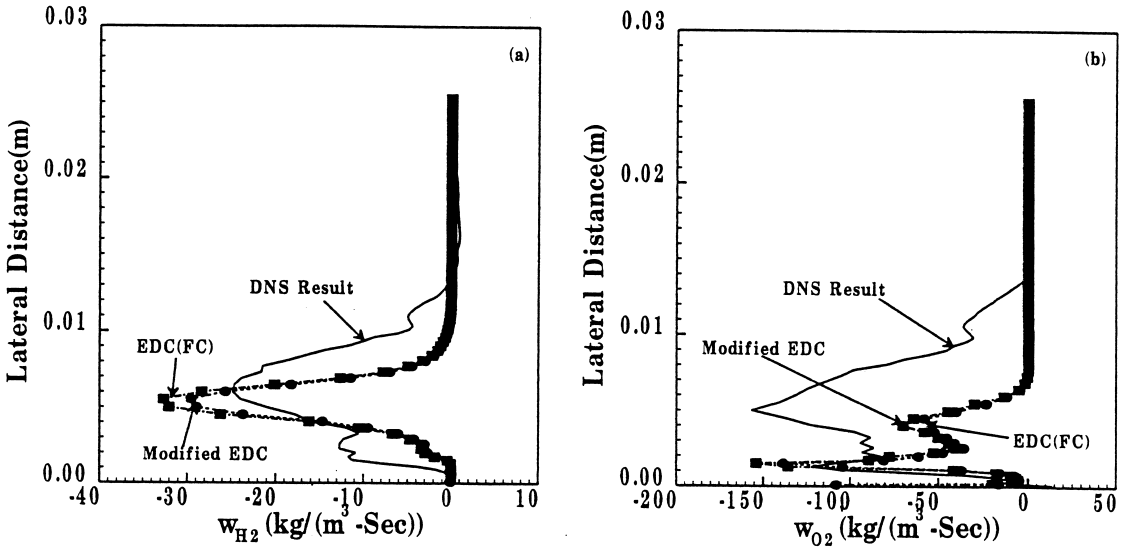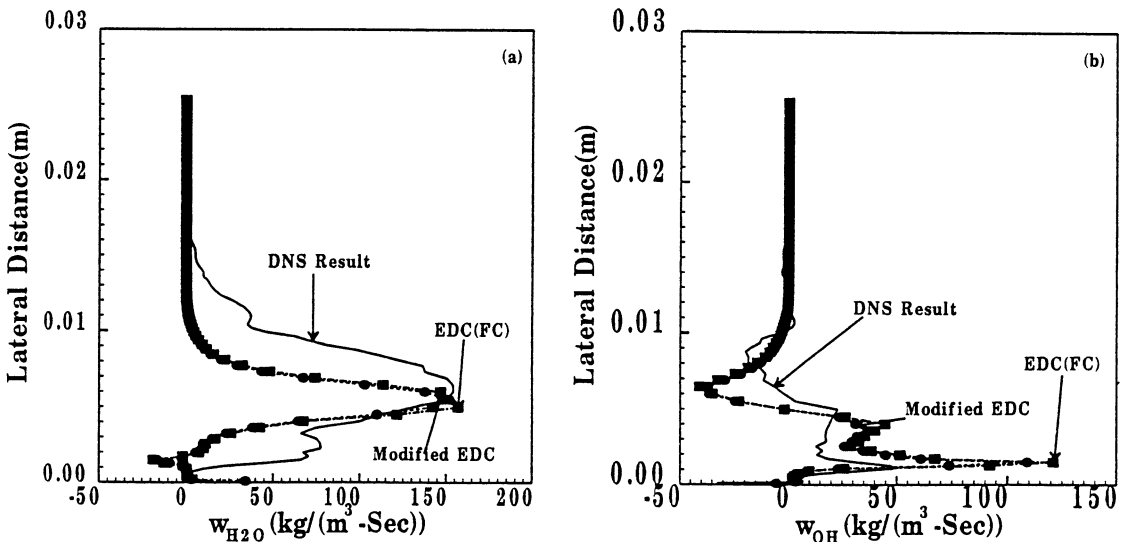
Fig. 5. Comparison of species production rate profiles for case 1 between DNS results and the EDC (FC) models at $x = 0.5$ m. (a) H_2, (b) O_2.

son is not good for the upper side (H_2) of the mixing layer. Although the orders of the mean reaction rates predicted by the two are same, the model predicts a thinner reaction zone as in the previous case. Also the profile predicted by the model is not as smooth as the profiles of case 1. Because of the high momentum ratio of the two streams in the inflow plane, there is a shift in the general structure of the mixing layer

towards the upper wall. The grid used in the simulation is very fine only near the interface and the wall boundary layers but relatively coarse in other zones. In this case, because of the shift of the structures, the flow development and the reaction occur in the zones where a relatively coarser grid is employed. As a result the turbulent kinetic energy (k) and the rate of dissipation of turbulent kinetic energy (ϵ) re-

Fig. 6. Comparison of species production rate profiles for case 1 between DNS results and the EDC (FC) model at $x = 0.5$ m. (a) H_2O, (b) OH.
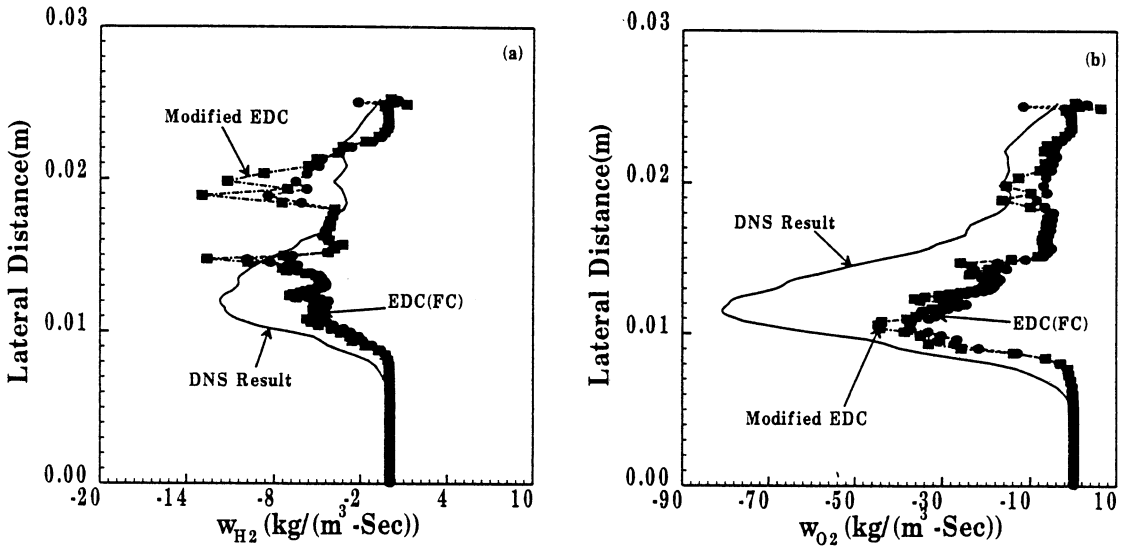
Fig. 7. Comparison of species production rate profiles for T = 1200 K between DNS results and the EDC (FC) model at x = 0.5 m. (a) H_2, (b) O_2.

quired for the model are not sufficiently resolved, particularly in the upper portion of the mixing layer. This fact can be viewed from the comparisons of the ϵ/k profiles for all the cases presented in Fig. 8. The profiles of ϵ/k for case 1 are much smoother than the profiles for case 2 and case 3. A finer grid in this zone may be required to have a better match. For the O_2 reaction rate, the model predicted much lower

peaks and thinner profiles compared to DNS results. H_2O and OH reaction rate profiles are compared in Fig. 9. As in the case of H_2 reaction rate, the comparisons are not very satisfactory in the upper portion of the mixing layer. The comparisons of the mean reaction rates of H_2, O_2, H_2O, and OH between DNS and the EDC (FC) model for case 3 are presented in Figs. 10 and 11 respectively.
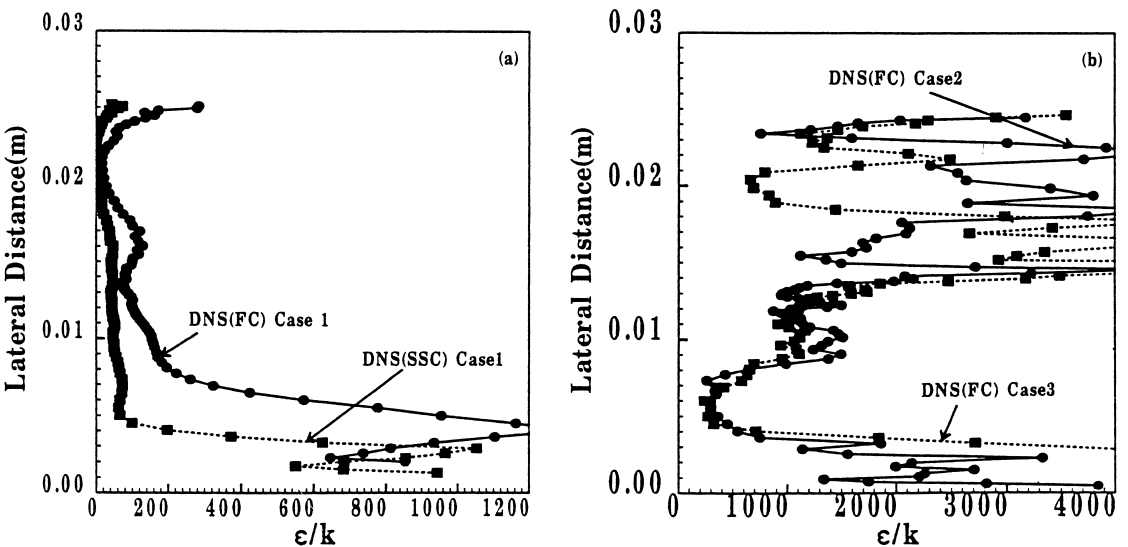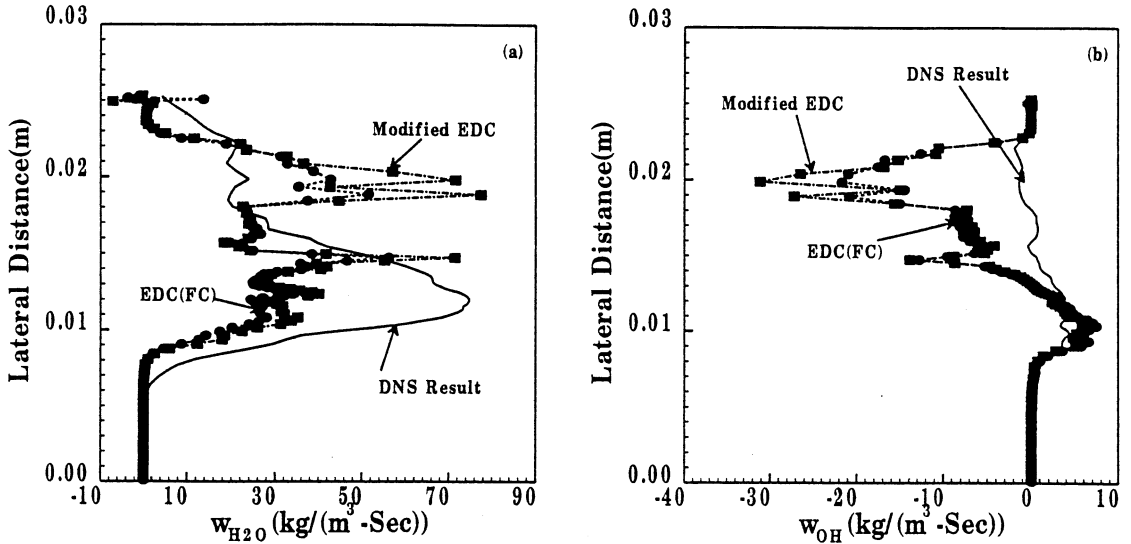

Fig. 8. Comparison of ϵ/k profiles at x = 0.5 m (a) between FC and SSC computations of case 1, (b) between FC for 1200 K and 1500 K.
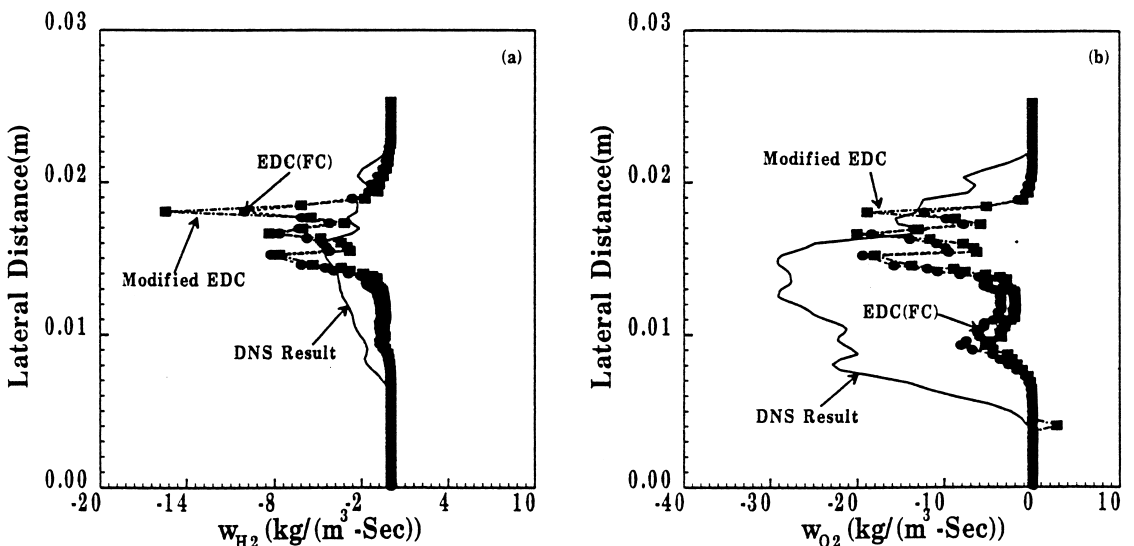
Fig. 9. Comparison of species production rate profiles for $T = 1200$ K between DNS results and the EDC (FC) model at $x = 0.5$ m. (a) H_2O, (b) OH.

To determine the predictive capability of the EDC (FC) model in the other regions of the flow field, transient data of all the fluid dynamical chemical variables are stored at the location of 0.1 m downstream of the splitter plate edge of the DNS (FC) results for the first case. As the ignition of the mixing layer is seen to occur at a distance of 0.04 m from the splitter plate edge [14], the comparisons of the mean reaction rate

profile at this station can help us to assess the performance of this model to predict the mean reaction rate in regions near the occurrence of ignition. The mean reaction rate profile comparison between DNS results and the EDC (FC) model for the axial location of 0.1 m is presented in Fig. 12 for the species H_2 and O_2; the comparison for the profiles of H_2O and OH is presented in Fig. 13. As earlier, the general

Fig. 10. Comparison of species production rate profiles for $T = 1500$ K between DNS results and the EDC (FC) model at $x = 0.5$ m. (a) H_2, (b) O_2.
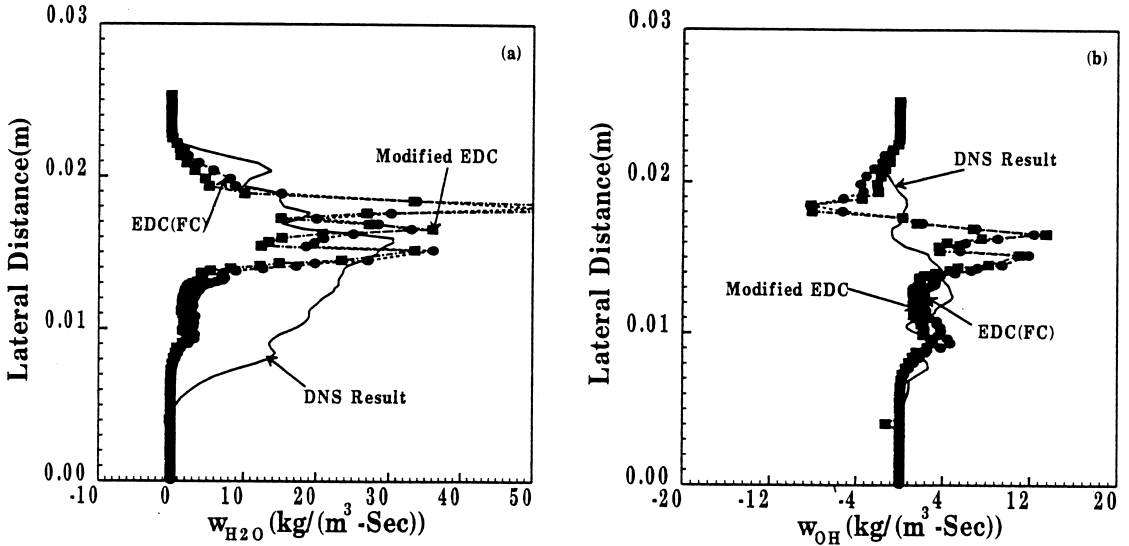
Fig. 11. Comparison of species production rate profiles for $T = 1500$ K between DNS results and the EDC (FC) model at $x = 0.5$ m. (a) H_2O, (b) OH.

shape of the profiles and the order of magnitude of the peak values between the two match fairly well except for the species O_2, although a thinner reaction zone is predicted by the model.

The comparisons of the EDC (FC) and EDC (SSC) results discussed so far have brought out clearly that the distribution of the reaction rate profiles of all the species are not as thick as the profiles obtained from the DNS results. The

cause of this departure was traced by comparing the nondimensionalized reaction rate parameter R_i (described in Eq. 13) from the DNS results and the EDC models. The computed nondimensionalized reaction rate parameters for the species $H_2(R_{H_2})$ from the DNS results of the various cases are plotted against the Reynolds number (Re_λ) based on Taylor length scale along with the value of R_{H_2} predicted by the
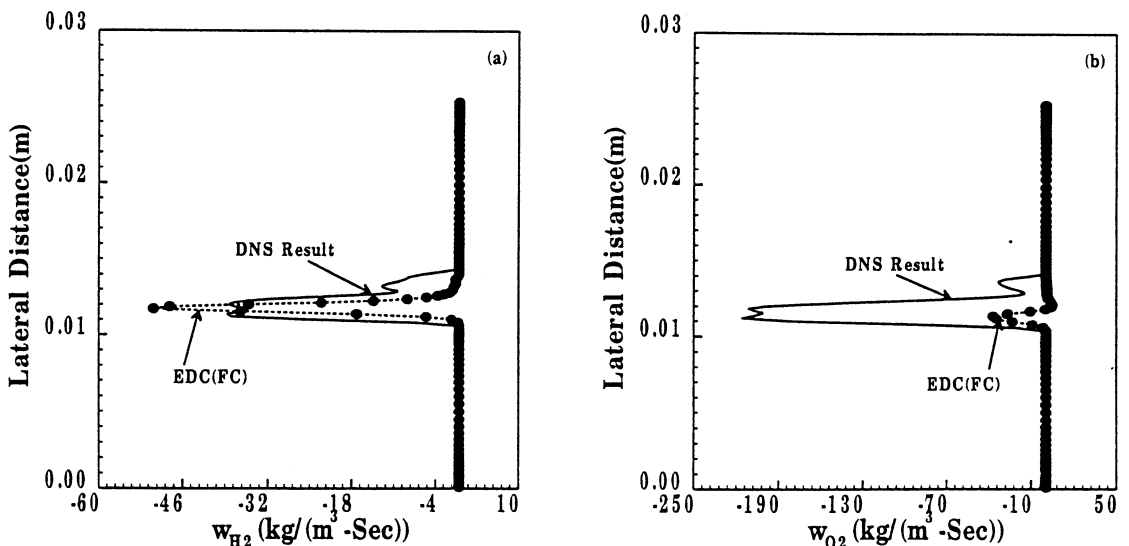

Fig. 12. Comparison of species production rate profiles for case 1 between DNS results and the EDC (FC) models at $x = 0.1$ m. (a) H_2, (b) O_2.
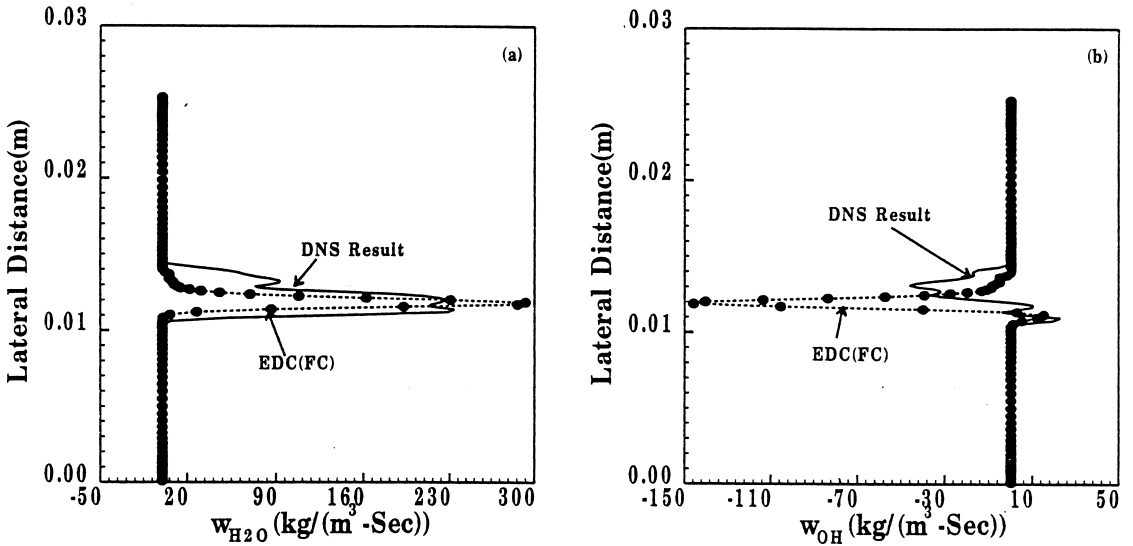
Fig. 13. Comparison of species production rate profiles for case 1 between DNS results and the EDC (FC) model at $x = 0.1$ m. (a) H_2O, (b) OH.

model in Fig. 14. It is very clear from the figure that for the higher Re_λ the computed R_{H_2} deviates much from the model value. The R_{H_2} computed from the EDC model is almost independent of Re_λ whereas the computed R_{H_2} dipped down for higher Re_λ. The correction for higher Re_λ is required in the EDC model to make it work better in the high-speed combusting flow.
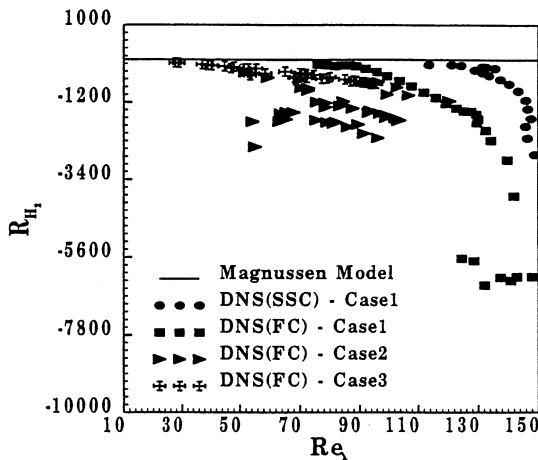

Fig. 14. Comparison of R_{H_2} between DNS results and EDC model.

CONCLUSIONS

Various empirical combustion models were evaluated for their predictive capability of mean reaction rate for the high-speed confined mixing layers using the time series data of DNS. The empirical model based on fast chemistry approximation cannot predict the mean reaction rate accurately. In the mixing layer region, where the reaction takes place, the models based on fast chemistry approximation show the mean reaction rate as high as two orders of magnitude compared to DNS data. The EDC models based on finite rate chemistry (both for FC and SSC) do well in predicting the mean reaction rate of the confined high-velocity mixing layer. The general shape of the reaction rate profile and the peak value computed from the EDC finite rate chemistry model match well with the DNS data at different locations of the flow field. The comparisons of the predicted mean reaction rates with different hydrogen and air stream temperatures with the DNS data also support this conclusion. For the hypervelocity reacting mixing layer, where the enthalpy change due to gas dynamics is significant compared to the enthalpy change due to chemistry, the finite rate EDC model seems to be adequate

to describe turbulence–chemistry interaction. It is worthwhile to fine tune the model for proper prediction of reaction zone width. This work is perhaps the first to test out the efficacy of such a model for supersonic flow. More effort in this direction is valuable to generate calculation methods for supersonic reacting flows.

REFERENCES

1. Givi, P., *Prog. Energy Combust. Sci*. 15:1–107 (1989).
2. Vervisch, L., and Poinsot, T., *Ann. Rev. Fluid Mech*. 30:655–691 (1998).
3. Bilger, R. W., in *Turbulent Reacting Flows* (P. A. Libby and F. A. Williams, Eds.), Springer-Verlag, 1980, Heidelberg, pp. 65–114.
4. Jones, W. P., and Whitelaw, J. P., *Combust. Flame* 48:1–26 (1982).
5. Borghi, R., *Prog. Energy Combust. Sci*. 14:245–292 (1989).
6. Spalding, D. B., *Thirteenth Symposium (International) on Combustion*, 1970, The Combustion Institute, Pittsburgh, pp. 649–657.
7. Magnussen, B. F., and Hjertager, B. H., *Sixteenth Symposium (International) on Combustion*, 1976, The Combustion Institute, Pittsburgh, pp. 719–729.
8. Gran, I. R. (1994). Ph.D. dissertation, University of Trondheim, Trondheim, Norway.
9. Pope, S. B., *Prog. Energy Combust. Sci*. 11:119–192 (1985).
10. Eiffer, P., and Kollmann, W., (1993). AIAA Paper 93-0448.
11. Zheng, L. L. (1993). Ph.D. dissertation, Cambridge University, Cambridge, U.K.
12. Girimaji, S. S., *Combust. Sci. Technol*. 78:177–196 (1991).
13. Girimaji, S. S. (1991). AIAA Paper 91-1792.
14. Chakraborty, D., Nagraja Upadhyaya, H. V., Paul, P. J., and Mukunda, H. S., *Phys. Fluids* 9:3513–3522 (1997).
15. Nagraja Upadhaya, H. V., Chakraborty, D., Paul, P. J., and Mukunda, H. S., *Proceedings of the XV National Conference on I.C. Engines and Combustion*, Chennai, India, 1997, pp. 693–700.
16. Erdos, J., Tamagno, J., Bakos, R., and Trucco, R. (1992). AIAA-92-0628.
17. Clemens, N. T., and Mungal, M. G. (1990). AIAA-90-1978.
18. Ragab, S. A., and Wu, J. L., *Phys. Fluids A* 1:957–966 (1989).
19. Sandham, N. D., and Reynolds, W. C., *AIAA J*. 28: 618–622 (1990).
20. Tam, C. K. W., and Hu, F. Q., *J. Fluid Mech*. 203:51–76 (1989).
21. Zhuang, M., Dimotakis, P. E., and Kubota, T., *Phys. Fluids A* 2:599–604 (1990).
22. Papamoschou, D., and Roshko, A., *J. Fluid Mech*. 197:453–457 (1988).
23. Lu, P. J., and Wu, K. C., *Phys. Fluids A* 3:3063–3069 (1991).
24. Shin, D. S., and Ferziger, J. H., *AIAA J*. 31:677–685 (1993).
25. Drummond, J. P., Carpenter, M. H., and Riggins, D. W., in *High Speed Flight Propulsion System*, (S. N. B. Murthy and E. T. Curran, Eds.), *Progress in Aeronautics and Astronautics*, Vol. 137, 1991.
26. Sekar, B., and Mukunda, H. S., *Twenty-Third Symposium (International) on Combustion*, The Combustion Institute, Pittsburgh, 1990, pp. 707–713.
27. Mukunda, H. S., *Combust. Sci. Technol*. 89:285–290 (1992).
28. Carpenter, M. H., and Kamath, H. (1988). *Three Dimensional Extension of the SPARK Combustion Code*. NASA-Langley, NASA-CP-5029, pp. 107–137.
29. Carpenter, M. H. (1988). *A Generalized Chemistry Version of SPARK*. NASA-CR-4196.
30. Bilger, R. W., *Combust. Sci. Technol*. 13:155–170 (1976).
31. Brizuela, E. A., and Bilger, R. W., *Combust. Flame* 104:208–212 (1996).
32. Magnussen, B. F., *Eighteenth International Congress on Combustion Engines*, International Council on Combustion Engines, Tianjin, China 1989.
33. Tennekes, H., and Lumley, J. K., *A First Course in Turbulence*, MIT Press., Cambridge, MA, 1972.